International Journal of the Korean Society of Precision Engineering, Vol. 3, No. 3. July 2002.

Dynamic Analysis on Belt-Driven Spindle System of Machine Tools

Seong Keol Kim

Graduate School of Automotive Engineering, Kookmin University, Seoul, Korea

ABSTRACT

The need of ultra-precision machine tools, which manufacture and machine the high precision parts used in computers, semi-conductors and other precision machines, has been increased over years. Therefore it is important to design the driving parts, which affect significantly on their performances. In this paper, the dynamic analyses on the belt-driven system were explored. Relation of the acoustical natural frequency and the tension of belt was derived and presented through experiments. Also, while the dynamic loads on motor system were changed, dynamic deflections were calculated through finite element analysis. Nonlinear characteristics of the bearings having an effect on the dynamic performance were studied and the belt connecting the motor (driving part) to spindle of a machine tool (driven part) was modeled as truss and beam elements for simulations under various conditions, and a beam element model was verified to be more useful.

Keywords : Ultra-precision machine tools, Driving part, Belt-driven system, Acoustical natural frequency, FEM, Nonlinear characteristics

1. Introduction

Recently, nano-scaled precision has been needed in the fields of computer, semi-conductor and precision machines. Therefore, the importance of design of ultra-precision machine tools, which machines precision parts, is getting increased, especially the driving parts. Since surface roughness and shape error are critical factors in ultra-precision parts, and those are significantly effected by dynamic characteristics of main spindle system, dynamic performance of driving part is very important. Generally, driving part is directly connected to the main spindle system and is driving the ultra-precision machine tools[1].

Only a few companies in USA, Japan and Europe are currently producing the ultra-precision machine tools, and researches on them are not so many. In domestic situation, need for ultra-precision machined parts of laser printer and camcorder is large, however almost most of them are depending on imports, and a few domestic machined parts also are manufactured by imported machine tools. Since technologies relating to ultra-precision machine tools in USA and Japan are very high valued, they do not want transfer of their technologies. Therefore, we should study and research this filed.

Generally, there are two ways to transmit dynamic power of main spindle in ultra-precision machine tools. The first is a way to connect motor to spindle directly by non-contacting coupling (magnetic coupling), and the second is that motor and main spindle are separated and transmit dynamic power by belt. In this paper, I focused on a study on belt-driven way. In order to analyze the belt-driven spindle system, experiments of belt tension measurement and dynamic simulations by FEM should be performed, and I strongly believe that those results would be basic design data of ultra-precision machine tools.

2. Determinations of belt tension and its equivalent stiffness

2.1 Measurement of belt tension

2.1.1 Experimental way and set-up

Performance and life of belt depend on belt tension[3]. Larger belt tension generates overload on bearing, and reduces lives of belt and bearing. However smaller belt tension generates slipping phenomenon, and wears belt quickly. Among measuring ways of belt tension, experimental function[3] was used, and this was constructed from relation of tension and the 1st acoustical natural frequency. In experimental instruments, Kravis tension-meter was replaced by microphone. In Figures 1 and 2, experimental set-up is shown.

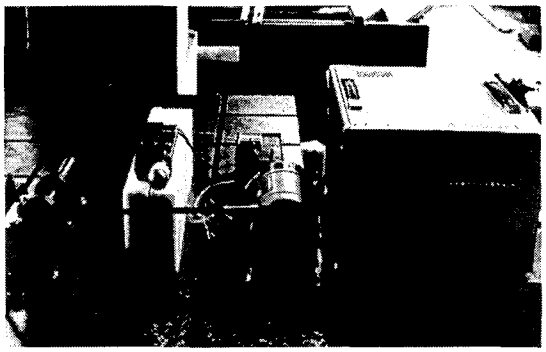

Fig. 1 Measurement of belt tension by microphone

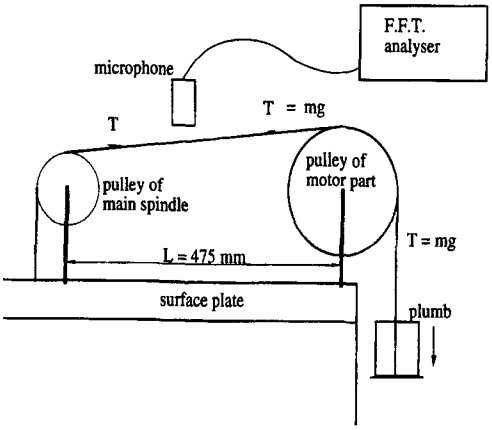

Fig. 2 A schematic of experimental set-up

This test is executed as follows; first, belt is impacted by screw driver, and the acoustical signals are measured by microphone. And the first acoustical natural frequency is calculated by using FFT analyzer. Second, as plumbs of mass equivalent to various belt tensions are used and changed to 15.9, 20.9, 25.9, 30.9, and 35.9 kgs, the 1st and the 2nd natural frequencies are measured for each plumb of mass. The length of V-belt used in the test is 475.0 mm, and thickness, outside width and inside width of belt are 8.5, 12.0 and 6.5 mms, respectively. Cross sectional shape of this V-belt is trapezoid.

2.1.2 Results

The 1st acoustical natural frequencies are shown in Table 1, and those results are measured for 5 loads.

Table 1 Results of test by changing mass of plumb

Mass (kg)	1st natural frequency
15.9	46.0
20.9	52.4
25.9	56.5
30.9	62.3
35.9	66.5

To derive relation of the tension and the 1st natural frequency obtained from above test, curve fitting program was written by FORTRAN 77, and the equation has a form like equation (2). This equation is a little different from equation (1) by J. N. Fawcett[2].

$$T = A + B f^2 \tag{1}$$

$$T = A_0 + A_1 f + A_2 f^2 \tag{2}$$

Values of each coefficient are like; A_0=-70.949, A_1=1.620 and A_2=0.071, and the results are shown in Fig. 3.

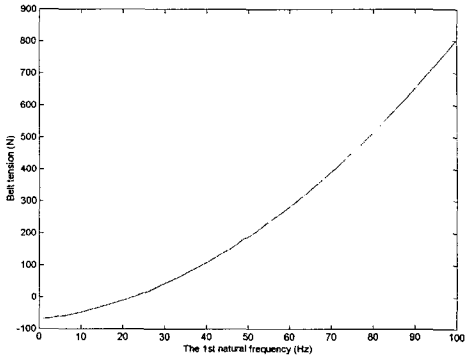

Fig. 3 Relation of belt tension and the 1st natural frequency

2.1.3 Discussion of test results

By using microphone, the function of belt tension was built for the 1st natural frequency, and relation of the tension and the 1st acoustical natural frequency was derived. Also, this was verified to be useful way to measure the tension.

2.2 Tension tests

2.2.1 Experimental way and set-up

To build the belt model by changing tension as preliminary test for FEM analysis, tension tests were performed for two types of belts. The one is flat belt, and width and thickness are 30.0 and 4.8 mms, respectively. The other one is V-belt used in previous section. Tests were executed by changing the length of belt to 300, 400 and 450 mms for each belt. As results of tests, relations of the tension and deflection of each belt were obtained. In Fig. 4, tension test se-up of V-belt is shown.

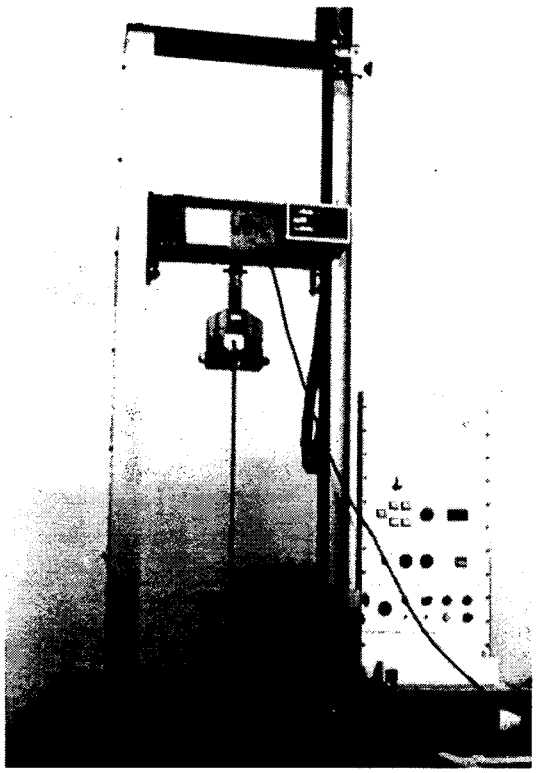

Fig. 4 Tension test set-up of V-belt

2.2.2 Test results

In tension tests for each length of a belt, relations of tension and deflection were measured and those data were obtained by plotter connected to tension testing machine. Among the data, more data were taken in smaller tension range to derive function of tension and deflection of belt. Curve fitting program was also used, and shapes of function for each belt are like;

$$\text{Flat belt}: \quad T = A_0 + A_a\delta + A_2\delta^2 \tag{3}$$

$$\text{V-belt}: \quad T = A_0 + A_a\delta + A_2\delta^2 + A_3\delta^3 + A_4\delta^4 \tag{4}$$

In below Tables and Figures, each coefficient of the second order function for flat belt and each coefficient of the forth order function are shown.

Table 2 Coefficients of function for flat belt

Function	$T = A_0 + A_a\delta + A_2\delta^2$		
Length	Coefficients		
	A_0	A_1	A_2
300 (mm)	-0.95	26.4	0.78
400 (mm)	-2.25	22.4	0.45
450 (mm)	-.265	19.0	0.35

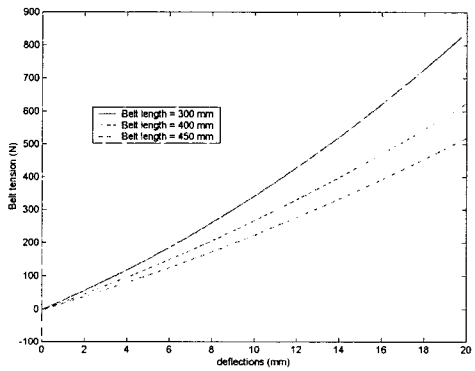

Fig. 5 Relation of tension and deflections for flat belt

Table 3 Coefficients of function for V-belt

Function	$T = A_0 + A_a\delta + A_2\delta^2 + A_3\delta^3 + A_4\delta^4$				
Length	Coefficients				
	A_0	A_1	A_2	A_3	A_4
300 (mm)	-5.84	154.8	12.93	-3.91	0.23
400 (mm)	-11.07	137.4	9.37	-2.46	0.13
450 (mm)	-19.73	75.57	15.02	-2.28	0.09

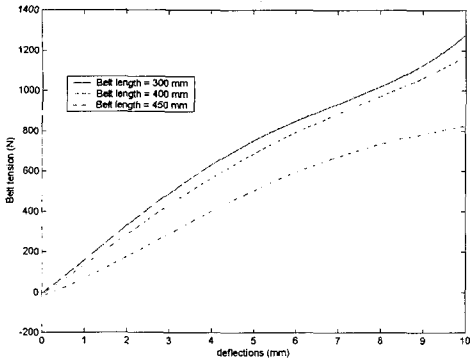

Fig. 6 Relation of tension and deflection for v-belt

To construct FEM model, equivalent stiffnesses of each belt were analyzed as followed, and variations of equivalent stiffnesses by changing length are shown in Table 4.

Equivalent stiffness of flat belt

$$T = A_0 + A_a\delta + A_2\delta^2$$

$$T/\delta = (k_{fb})_{eq} = (A_0 + A_a\delta + A_2\delta^2)/\delta = EA/L \quad (5)$$

L : Length of belt

A : Cross sectional area (144.64 mm^2)

E : Equivalent elastic modulus of flat belt by equation (5)

Equivalent stiffness of V-belt

$$T = A_0 + A_a\delta + A_2\delta^2 + A_3\delta^3 + A_4\delta^4$$

$$(k_{fb})_{eq} = (A_0 + A_a\delta + A_2\delta^2 + A_3\delta^3 + A_4\delta^4)/\delta = EA/L \quad (6)$$

E : Equivalent elastic modulus of V-belt by equation (6)

Table 4 Equivalent stiffness and elastic modulus of each belt at T=300 N

Type	V-belt		Flat belt	
Length (mm)	Equiv. stiff. (kN/m)	Elastic m. (MN/m^2)	Equiv. stiff. (kN/m)	Elastic m. (MN/m^2)
300	163.7	624.6	32.34	69.17
400	142.1	723.4	26.07	74.86
450	97.0	555.2	22.30	72.52

2.2.3 Discussion of the test results

Relations of tension and deflection for each belt were verified. As the results, V-belt was a shape of the 4th order function, and flat-belt was a shape of the 2nd order function. Also, through experimental functions for each belt, equivalent stiffnesses for FEM model were obtained.

3. Numerical analysis of belt-driven system

3.1 Modeling of belt-driven main spindle

In order to simulate belt-driven system, not only belt but also motor, main spindle and pulley should be analyzed simultaneously[3-6]. In this study, belt driven main spindle system was divided into 3 sub-systems, motor, belt pulley and main spindle, and was modeled to analyze FEM. Dynamic deflection analysis was performed for changing dynamic load. In FEM model, x-axis is a direction of main spindle and motor spindle, and z-axis is a direction of belt. FEM modeling of belt-driven main spindle system is shown in Fig. 7.

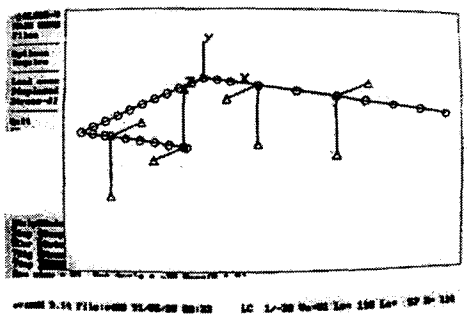

Fig. 7 Modeling of belt-driven main spindle system

3.1.1 Modeling of motor

In Fig. 8, a schematic of modeling of motor is shown. Belt tension, T was modeled to –y-direction, and also pulley weight was modeled as a concentrated mass to +z-direction at left end of motor. Nodes of motor spindle were 11, and its elements were 9. Physical properties are shown in Table 5.

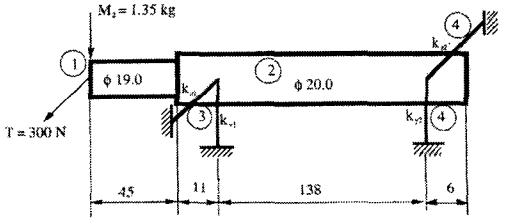

Fig. 8 Modeling of motor

A type of ball bearing supporting motor was NSK single raw deep groove bearing (6204zz, 6304zz).

Table 5 Physical properties of motor system

	Section 1	Section 2
Diameter D (mm)	19.0	20.0
Cross sectional area A (mm^2)	283.53	314.16
Moment of inertia (mm^4)	6,397.1	7,854.0
Polar moment of inertia (mm^4)	12,794.1	15,708.0

Each bearing was modeled as two truss elements, and total truss was 4. Therefore, nodes were 4, and cross sectional shapes were 4. Directions of each truss element were determined by considering real loaded conditions of each bearing. Y-directional loads were masses of motor spindle(distributed mass) and pulley(concentrated mass), and z-directional load was belt tension(T). By using relation of deflection and load working on bearing, numerical program[7] was written by FORTRAN 77. Length of truss element was fixed to 10.0 mm, and Young's modulus was also fixed to 2.0×10^{11} N/m^2. $(k_b)_{eq}$ was determined by equation (7).

$$(k_b)_{eq} = \frac{F}{\delta} = \frac{EA}{L} \tag{7}$$

Equivalent stiffness of bearing obtained in numerical analysis was put into equation (5), and cross sectional area (A) was determined for the $(k_b)_{eq}$. Among calculated bearing stiffnesses, k_{y1} and k_{y2} are constant since masses of motor spindle and pulley are fixed to constant, however, k_{z1} and k_{z2} are changed by belt tension.

3.1.2 Modeling of main spindle

A schematic of modeling of main spindle is shown in Fig. 9. In this modeling, pulley at left end was modeled as –y-directional concentrated mass, and tension (T) was modeled as +z-directional concentrated mass. Nodes of main spindle were 11, and it was modeled as beam with 9 elements. Physical properties are shown in Table 6.

A type of ball bearing supporting main spindle was FAG self-aligning ball bearing. Each bearing was modeled as two truss elements like the bearing supporting motor at section 3.1.1. Also, directions of truss elements were determined through real loaded conditions of bearings. Therefore, masses of main spindle(distributed mass) and pulley(concentrated mass) were modeled to y-direction, and belt tension was modeled to z-direction. $(k_b)_{eq}$ of main spindle was determined by the same way of section 3.1.1.

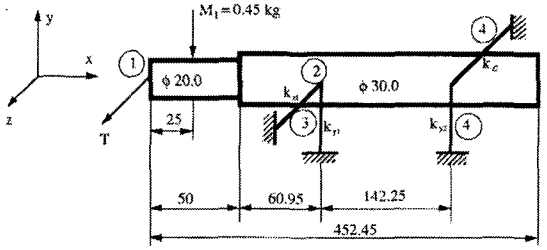

Fig. 9 Modeling of main spindle

Table 6 Physical properties of main spindle system

	Section 1	Section 2
Diameter D (mm)	20.0	30.0
Cross sectional area A (mm^2)	314.16	706.86
Moment of inertia (mm^4)	7,854.0	39,760.8
Polar moment of inertia (mm^4)	15,708.0	79,521.6

3.1.3 Modeling of belt

Belt was modeled as a beam element and a truss element, and the validity of each model was explored. When belt was modeled as a truss, $(k_b)_{eq}$ was through tension test, and was assumed that n equivalent springs were connected to be serial when n elements were used. Since in equation (5), belt length (L), cross sectional area (A) and $(k_b)_{eq}$ were already known, equivalent elastic modulus (E) could be calculated, and is shown in Table 4.

When belt was modeled as a beam, E was the same value as modeling of truss element, and belt was remodeled as equivalent circular beam element having the same cross sectional area (A) of a belt. To obtain cross sectional area of belt, equivalent diameter of belt (D) was calculated from equation (8), and x and y-directional moments of inertia were obtained from equation (9). Z-directional polar moment of inertia was from equation (10).

$$A = \frac{\pi}{4}D^2 \tag{8}$$

$$I_{xx} = I_{yy} = \frac{\pi}{64}D^4 \tag{9}$$

$$I_{zz} = \frac{\pi}{32}D^4 \tag{10}$$

3.2 Results of simulations

For 2 types of belts, belt was modeled as a beam and a truss. And dynamic deflections were simulated through FEM for changing dynamic loads. Dynamic loads for the simulations were calculated from equation (11), and these loads were worked on to y and z directions.

$$F = me\omega^2 \sin \omega t \quad (11)$$

where

m : unbalanced mass of motor

e : eccentricity

ω : revolutions per minute

Conditions of simulations are as follows; time interval, Δt is 0.002 second, and time steps are 41. In Figures 10~13 and Tables 7~9, Results of simulation are shown at fixed belt tension (T=300N).

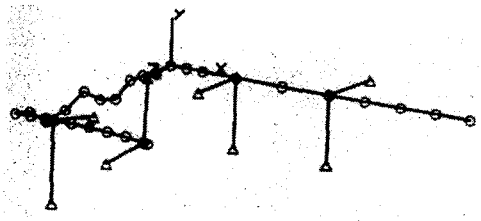

Fig. 10 Results of simulation I (T=300N, L=400 mm) for V-belt

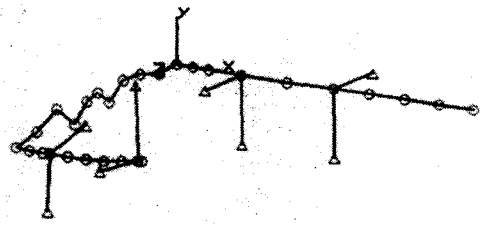

Fig. 11 Results of simulation II (T=300N, L=450 mm) for V-belt

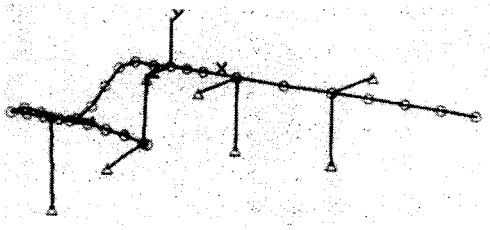

Fig. 12 Results of simulation III (T=300N, L=400 mm) for flat belt

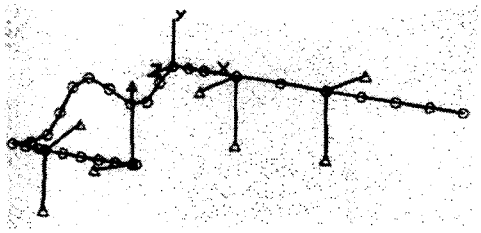

Fig. 13 Results of simulation IV (T=300N, L=450 mm) for flat belt

3.3 Discussions of the simulation results

Through FEM analysis, I have five results as follows. First, through tension test, flat belt is proved to be more flexible than V-belt. Also, as belt is more flexible, and belt length is longer, the deflections of right end of main spindle (driven) are found to be smaller. Second, when belt is modeled, beam element is proved to be more useful than truss element through the results of dynamic simulations. As shown in Table 7, when dynamic load of equation (11) is applied to y and z-directions of motor system, in case of using truss element, only z-directional deflections normal to cross section of belt are came out, since truss element works like a linear spring. However, in case of using beam element, all of directional deflections are found. Third, as dynamic load working on motor system increases, the deflections of right end of main spindle increase. Fourth, as belt tension increase, x-directional deflections of right end of main spindle increase, however, z-directional deflection decreases. Since equivalent stiffness of ball bearing is nonlinearly proportional to working load, larger tension means increase of z-directional stiffness. Fifth, through above results, the effectiveness of vibration isolation by belt is found to be very large. When main spindle with air bearing is used in ultra-precision machine tools, to minimize the influence of vibration of motor system, I propose that longer belt length and smaller tension at allowable space are used.

4. Conclusions

In order to design driving system of precision machine tools, belt-driven main spindle system was constructed. Also, tests and simulations were performed for this system. As preliminary tests, tension measuring test and tension test to derive equivalent stiffnesses for two types of belts were executed. By using the acquired

Table 7 Results of dynamic simulations at F=10N and T=300N

(a) V-belt (μm)

Modeling / Direction / Length	Truss element						Beam element					
	Left end of motor			Right end of spindle			Left end of motor			Right end of spindle		
	x	y	z	x	y	z	x	y	z	x	y	z
300 (mm)	0.0	3.663	1.192	0.0	0.0	0.025	0.187	3.663	2.440	0.159	0.003	0.007
400 (mm)	0.0	3.664	1.230	0.0	0.0	0.003	0.131	3.941	2.243	0.083	0.003	0.013
450 (mm)	0.0	3.664	1.232	0.0	0.0	0.002	0.062	3.663	2.461	0.074	0.009	0.004

(b) Flat belt (μm)

Modeling / Direction / Length	Truss element						Beam element					
	Left end of motor			Right end of spindle			Left end of motor			Right end of spindle		
	x	y	z	x	y	z	x	y	z	x	y	z
300 (mm)	0.0	3.664	1.234	0.0	0.0	0.001	0.071	3.664	2.491	0.066	0.002	0.002
400 (mm)	0.0	3.663	1.234	0.0	0.0	0.001	0.077	3.943	2.289	0.058	0.003	0.035
450 (mm)	0,0	3.665	1.234	0.0	0.0	0.001	0.055	3.665	2.501	0.050	0.001	0.016

Table 8 Results of dynamic simulations by beam element of belt at F=10, 50, 100, 400N, T=300N and L=400mm

(μm)

Belt type / Direction / F (N)	V-belt						Flat belt					
	Left end of motor			Right end of spindle			Left end of motor			Right end of spindle		
	x	y	z	x	y	z	x	y	z	x	y	z
10	0.131	3.941	2.243	0.083	0.003	0.013	0.077	3.943	2.289	0.058	0.003	0.004
50	0.643	18.32	12.23	0.408	0.008	0.029	0.379	18.32	12.49	0.284	0.009	0.008
100	1.308	39.42	22.43	0.835	0.004	0.127	0.765	39.43	22.89	0.578	0.029	0.036
400	5.144	146.5	97.81	3.267	0.065	0.232	3.028	146.6	99.90	2.276	0.074	0.065

Table 9 Results of dynamic simulations by changing belt tension at F=10N and L=400mm

(μm)

Belt type / Direction / Tension (N)	V-belt						Flat belt					
	Left end of motor			Right end of spindle			Left end of motor			Right end of spindle		
	x	y	z	x	y	z	x	y	z	x	y	z
50	0.895	36.63	35.72	0.708	0.017	0.346	0.514	36.64	36.54	0.490	0.018	0.119
100	1.052	36.63	30.56	0.741	0.017	0.213	0.578	36.64	31.26	0.505	0.018	0.066
200	1.168	36.63	26.35	0.763	0.016	0.113	0.658	36.64	26.94	0.521	0.018	0.032
300	1.308	39.42	22.43	0.835	0.004	0.123	0.765	39.43	22.89	0.578	0.029	0.036

experimental data, FEM analysis of belt-driven main spindle system was executed. For FEM modeling of belt-driven system, it was divided into motor, belt and main spindle. Since equivalent stiffnesses of bearings supporting motor and main spindle were changed nonlinearly by load working on bearings, a program considering nonlinearity of bearing from above relation was written. Equivalent stiffnesses were found by changing load working on bearing, and it was modeled as a truss element. Dynamic deflection analysis was performed by changing eccentric load which resulted from unbalanced mass of motor.

Belt was modeled as a beam and a truss. As the results of simulations, a beam model was verified its

validity. Under the condition of constant equivalent stiffness of bearing, longer belt length and smaller tension showed larger vibration isolation.

Acknowledgement

This work was supported by the Brain Korea 21 Project in 2002.

References

1. Cheong, I. S., Je, J. S., and In, D. S., "A study on the Vibration Characteristics of V-belt Driving System," Journal of the Korean Society of Mechanical Engineers, Vol. 6, pp. 93-99, 1982.
2. Fawcett, J. N., Burdess, J. S., and Hewit, J. R., "Belt Natural Frequency as an Indicator of Belt Tension," Proceedings of the 1989 International Power Transmission and Gearing Conference, ASME, pp. 25-29, 1989.
3. Wang, K. W., "Dynamic Stability Analysis of High Speed Axially Moving Bands with End Curvatures," Journal of Vibration and Acoustics, Vol. 113, pp. 62 - 68, 1991.
4. Gerbert, G., "Tooth Action in Chain and Timing Belt Drives," Proceedings of the 1989 International Power Transmission and Gearing Conference, ASME, pp. 81-89, 1989.
5. Wang, K. W., and Mote, C. D. Jr., "Vibration Coupling Analysis of Band/Wheel Mechanical Systems," Journal of Sound and Vibration, Vol. 109, pp. 237-258, 1986.
6. Perkins, N. C., "Linear Dynamics of a Translating String on a Elastic Foundation," Journal of Vibration and Acoustics, ASME, Vol. 112, pp. 2-7, 1990.
7. Kim, S. K., "A study on the Analysis of Dynamic Characteristics of Main Spindle Considering Nonlinear Characteristics of Bearing," Master Thesis, Seoul National University, 1988.